Spectral Dimensionality and Scale of Urban Radiance

Christopher Small

Lamont Doherty Earth Observatory
Columbia University
Palisades, NY 10964 USA
small@LDEO.columbia.edu

Abstract

Characterization of urban radiance and reflectance is important for understanding the effects of solar energy flux on the urban environment as well as for satellite mapping of urban settlement patterns. Spectral mixture analyses of Landsat and Ikonos imagery suggest that the urban radiance field can very often be described with combinations of three or four spectral endmembers. Dimensionality estimates of AVIRIS radiance measurements of urban areas reveal the existence of 30 to 60 spectral dimensions. The extent to which broadband imagery collected by operational satellites can represent the higher dimensional mixing space is a function of both the spatial and spectral resolution of the sensor. AVIRIS imagery offers the spatial and spectral resolution necessary to investigate the scale dependence of the spectral dimensionality. Dimensionality estimates derived from Minimum Noise Fraction (MNF) eigenvalue distributions show a distinct scale dependence for AVIRIS radiance measurements of Milpitas, California. Apparent dimensionality diminishes from almost 40 to less than 10 spectral dimensions between scales of 8000 m and 300 m. The 10 to 30 m scale of most features in urban mosaics results in substantial spectral mixing at the ~20 m scale of high altitude AVIRIS pixels. Much of the variance at pixel scales is therefore likely to result from actual differences in surface reflectance at pixel scales. Spatial smoothing and spectral subsampling of AVIRIS spectra both result in substantial loss of information and reduction of apparent dimensionality, but the primary spectral endmembers in all cases are analogous to those found in global analyses of Landsat and Ikonos imagery of other urban areas.

Introduction

Recent estimates indicate that over 45% of the world's human population now lives in urban areas with over 60% projected by 2030 (*United Nations, 1999*). As the size and number of urban agglomerations increases, so does the relative importance of the urban environment to the global population. Remote sensing can serve (at least) two important roles in the study of the urban environment. Moderate resolution, broadband optical sensors on the Landsat and Spot satellites provide a 30 year time series with which to quantify urban growth and settlement patterns worldwide. In order to map urban growth with optical sensors, it is necessary to distinguish the reflectance properties of the urban surfaces from those of other landcover types. This is an inherently difficult task because urban areas incorporate spectrally identical land covers from other environments and because built urban surfaces are often composed of materials extracted from nearby surroundings. The scale and texture of urban reflectance is, however, often distinct from other landcovers so the combination of reflectance and textural properties is more informative. This requires a robust characterization of urban reflectance properties at different scales. The synoptic view of the urban mosaic provided by satellite and airborne sensors is also an important complement to *in situ* measurements of physical characteristics of the urban environment. The spectral reflectance properties of the urban mosaic have a strong influence on energy flux through the urban environment and the microclimatic variations that result (*Landsberg, 1981*). Since much of the reflectance of the built environment is subject to human modification, understanding

scale dependent optical properties of existing urban settlements may influence future design decisions. Characterization of urban spectral reflectance serves both of these objectives.

Analysis of reflectance properties in different urban environments may provide a basis for a general characterization of urban reflectance. Comparative analyses of Landsat and Ikonos imagery for a variety of cities worldwide indicates that spectral heterogeneity at scales of tens of meters is the most consistent characteristic of broadband spectral reflectance of urban areas (*Small, 2001b*). In spite of the lack of a single characteristic urban reflectance spectrum, almost all of the urban areas considered could be described as spectral mixtures of three or four endmembers as resolved by the Ikonos, Landsat TM and ETM+ sensors (*Small, 2001a*). In contrast, many of the areas surrounding these cities are characterized by more complex mixing spaces with larger numbers of spectral endmembers. Representation of urban reflectance with a simple spectral mixing model (e.g. *Adams et al, 1986, 1993; Smith et al, 1990; Gillespie et al, 1990*) would be desirable because it could accommodate the spectral heterogeneity with a physically based description consistent with the variety of reflectances observed in urban environments. This requires a more thorough understanding of the relationship between the true spectral dimensionality of the urban mosaic and the low dimensional projection of this mixing space that is resolved by broadband sensors like Landsat. The representation of the mixing space provided by broadband imagery is incomplete because these operational sensors lack the spectral resolution necessary to distinguish among materials with narrow absorption bands resolvable by imaging spectrometers like AVIRIS.

An analysis of high resolution AVIRIS imagery by *Green and Boardman, (2000)* found that a flight line collected of San Diego California had higher spectral dimensionality than datasets collected in other environments. This prompts the question of whether urban areas can really be characterized with simple linear mixing models or whether the true high spectral dimensionality of the urban mosaic will preclude development of a general characterization of urban reflectance. In order to resolve this question, it is necessary to consider the spatial scale of the observations. The objective of this analysis is to investigate the relationship between spatial scale and spectral dimensionality in an urban environment. The focus of the analysis in on the use of eigenvalue decomposition for multiscale estimation of spectral dimensionality.

Data and Analysis

This analysis used AVIRIS radiance and reflectance data collected over Milpitas California on 20 June 1997. These data are available as AVIRIS standard data products from *popo.jpl.nasa.gov*. The study area, shown in Figure 1, consists of undeveloped land, suburban residential areas and urban industrial areas. The primary spectral endmembers, derived from the analyses described below, are shown in Figure 2. These endmembers were selected using the methodology described by *Boardman (1993)* and *Boardman and Kruse (1994)*. Endmember spectra are shown in scaled reflectance for ease of interpretation, but all dimensionality estimates were made using calibrated radiance data so the information content is determined by both the surface reflectance characteristics and the atmospheric interactions.

Spectral dimensionality estimates are based on eigenvalue distributions obtained from principal component analyses as described by *Boardman and Green (2000)* and *Green and Boardman (2000)*. The Minimum Noise Fraction (MNF) transformation (*Green et al, 1988; RSI, 2000*) is used because it accommodates band-to-band differences in signal and noise amplitude and because the resulting eigenvalues provide an indication of the information and noise content of the data. All analyses shown here were done with ENVI image processing software. The MNF implemented in ENVI is similar to that Maximum Noise Fraction transformation described by *Green et al (1988)* but differs in the scaling of the resulting eigenvalues. The eigenvalues produced by ENVI's MNF are scaled in sigma noise units analogous to a signal-to-noise ratio so the number of eigenvalues greater than unity gives an estimate of

the number of dimensions with variance larger than the amplitude of the noise estimate. One advantage of the Minimum Noise Fraction transformation is that it accounts for the fact that the noise in some bands may be larger than the signal in other bands. Rather than basing the rotation on variance alone, the ENVI MNF attempts to "prewhiten" the data by performing an initial rotation to diagonalize the noise covariance and by rescaling the eigenvalues of the second rotation to sigma noise units (*RSI, 2000*).

In order to compare dimensionality estimates from different areas, it is necessary to use a consistent noise estimate. For this analysis, the noise estimate is based on a subimage acquired over the Calaveras reservoir in the same AVIRIS scene as the study area. By using the same noise covariance for all MNF rotations, differences in the resulting eigenvalue distributions should more accurately reflect differences in the signal content of each subscene. The noise covariance estimate is derived from differences in spectra of adjacent pixels so a dark, uniform target provides a crude approximation of a dark current noise source. The approximation is imperfect, however, because it includes actual differences in radiance related to spatial variations in surface reflectance and path radiance at scales of ~20 meters.

Figure 1. *AVIRIS false color composite of Milpitas California acquired in 1997. The Red, Green and Blue layers correspond to the 2.21 μm, 0.81 μm and 0.66 μm wavelength bands respectively. The image is 6 x 8 km and each pixel is approximately 20x20 m. The spectral dimensionality of the mosaic of urban, subruban and undeveloped areas varies at scales larger and smaller than the Ground Instantaneous Field Of View (GIFOV) of the AVIRIS sensor.*

Color image available from: *www.LDEO.columbia.edu/~small/Urban.html*

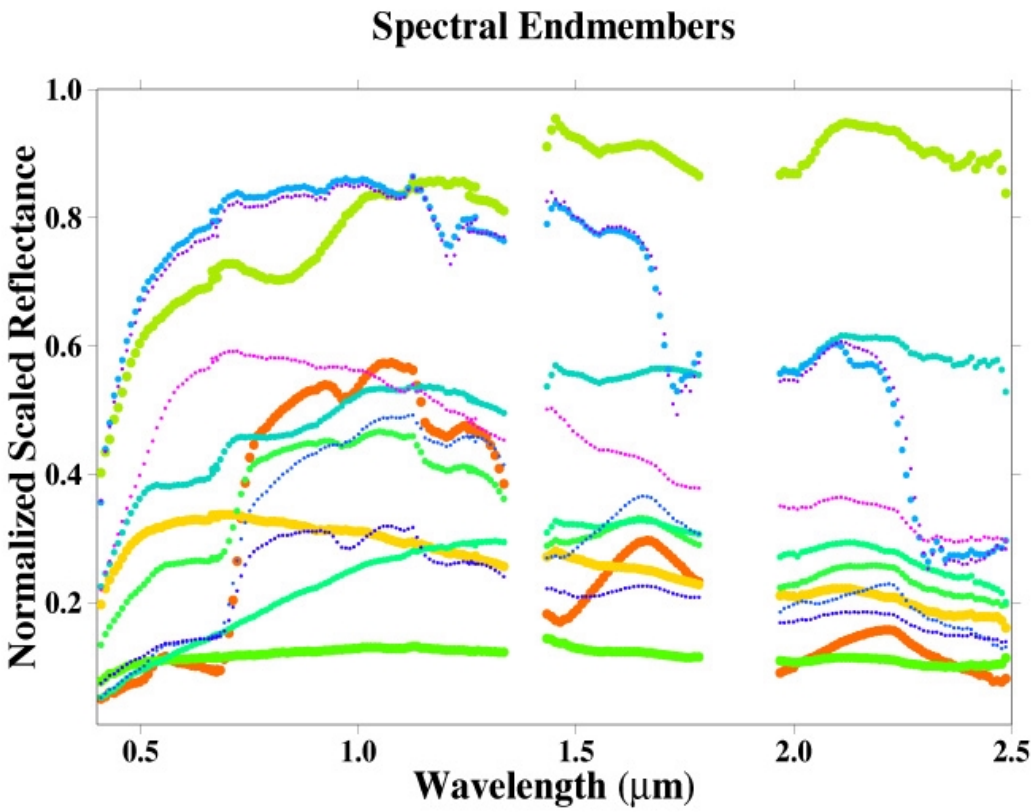

Figure 2. *Primary spectral endmembers for the AVIRIS reflectance image of Milpitas California. Spectra plotted with thicker curves and warmer colors are associated with the extrema of the low order dimensions of the mixing space. Thinner curves correspond to higher order dimensions. Each endmember is an average of 10 to 100 individual spectra residing at the apexes of the mixing space. The primary endmembers (high albedo, low albedo, soil and vegetation) span the mixing space of the three low order dimensions and describe 97.5% of the variance in a variance maximizing principal component rotation of the image. These endmembers are analogous to those found in spectral mixture analyses of other urban areas investigated with Landsat and Ikonos imagery. AVIRIS resolves many more distinct endmembers because the high spectral resolution discriminates subtle differences such as those seen in the different vegetation endmembers above.*

Color image available from: *www.LDEO.columbia.edu/~small/Urban.html*

The relationship between spatial scale and spectral dimensionality was quantified by comparison of 40 subscenes within the study area. Nine adjacent 100x100 pixel subscenes covering the built up area were used for the first stage of the analysis. Each of these ~2x2 km areas contained a variety of landcover types. Within these nine subscenes, ten 30x30 pixel subscenes were chosen in areas of undeveloped hillslopes, suburban residential and urban industrial development. An additional twenty 15x15 pixel subscenes allowed each of these landcover types to be further isolated in smaller areas.

Spatial averaging attenuates both noise and information to varying degrees while spectral resampling should preferentially attenuate the information content of the signal. The effects of spatial averaging and spectral resampling were tested in a 200x170 pixel subscene containing a combination of industrial and residential landcovers. Spatial averaging was done with a series of gaussian kernels ranging from 5x5 to 45x45 pixels. Spectral resampling was done using every Nth band of the original AVIRIS radiance dataset for N ranging from 2 to 16.

Results

Spectral endmembers bounding the mixing space of the lower order MNF dimensions are analogous to the endmembers found in analyses of other urban areas. Figure 2 shows 12 endmembers bounding the six primary dimensions of the mixing space. The endmember spectra bounding the lowest three dimensions correspond to vegetation, soil, high albedo roofing material and low albedo pavement. The endmembers spanning the low order dimensions are almost identical to those derived from a standard principal component analysis, indicating that a simple four component mixing model accounts for the vast majority of variance (97.5%) in the radiance field. The endmembers associated with the higher order dimensions are certainly significant but would not be resolved by broadband sensors.

The analysis of the 40 subscenes indicates a correspondence between area and dimensionality. When plotted in log-linear space, the eigenvalue distributions in Figure 3 all have a similar shape with a sharp break in slope separating the primary dimensions associated with higher, but rapidly diminishing, spatial autocorrelation from a long tail of gradually diminishing signal to noise levels. The break in slope corresponds to a transition from spatially coherent to spatially incoherent eigenimages. Figure 4 shows an example of this transition for a spectrally diverse subscene containing a variety of landcovers at different spatial scales. The transition from spatially coherent to spatially incoherent eigenimages occurs between dimension 31 and 35 but there are still isolated coherent features visible in these higher dimension eigenimages. These isolated features have distinct spectra and therefore represent useful information about the smaller features in the image.

The number of MNF eigenvalues larger than unity is often used as an indication of the inherent dimensionality of a hyperspectral image (e.g. *Boardman and Green, 2000, Green and Boardman, 2000, RSI, 2000*). Numerically, the eigenvalues larger than unity are associated with dimensions having variance greater than that of the noise estimate. In Figure 3, the eigenvalue distributions cluster in accordance with the size of the subimage. If the unity threshold is adopted, the results imply that the full image contains almost 200 spectral dimensions and that the 100x100 pixel subimages are also of comparable dimensionality. The apparent dimensionality drops somewhat for the 30x30 pixel subimages and more appreciably for the 15x15 pixel subimages. As pointed out by *Boardman and Green (2000)*, eigenvalue distributions are, however, merely a statistical proxy for dimensionality. In this study, the higher dimensions associated with the tail of the eigenvalue distribution do generally contain some small, spatially coherent features in the associated eigenimages that may correspond to distinct spectral features.

A more conservative criterion of spectral dimensionality would be the break in slope distinguishing the low order eigenvalues with coherent eigenimages associated with greater spatial coherence. This criterion also indicates a similar scale dependence in dimensionality. The full image and the 100x100 pixel subimages have transitions between 25 and 30 while the 30x30 pixel subimages have a transitions between 20 and 25. The 15x15 pixel subimages are small enough to contain more spectrally homogeneous areas and show a wide range of transitions between 10 and 25 dimensions. Using this "breakpoint" criterion, the hillslope subimages have the lowest dimensionality, and the suburban residential subimages have the highest dimensionality.

Spatial filtering of a high dimensional subscene results in both suppression of noise and dilution of spectral dimensionality. Figure 5 shows the eigenvalue distribution (labelled Raw) corresponding to the eigenimages shown in Figure 4. The raw image was smoothed with a succession of gaussian lowpass filters to investigate the effect of variance attenuation on the apparent dimensionality. The same unfiltered noise source was used for each MNF rotation. The effects of increased smoothing are 1) a successive reduction of variance (relative to the noise source) and 2) a shift in the breakpoint between the rapidly diminishing low-order eigenvalues and the gradually diminishing tail of higher order eigenvalues. The successive reduction in the number of eigenvalues greater than unity is a direct consequence of the

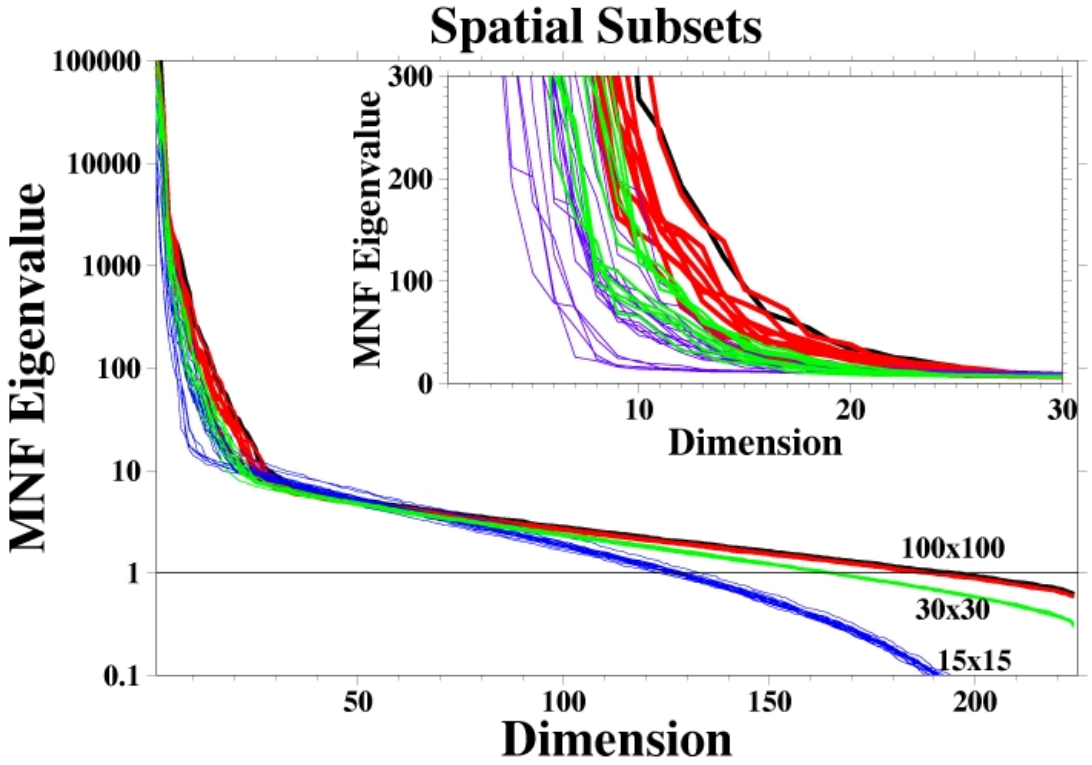

Figure 3. *Scale dependence of spectral dimensionality. The Minimum Noise Fraction (MNF) eigenvalue distributions correspond to spatial subsets of the AVIRIS image shown in Figure 1. The eigenvalues are scaled in sigma noise units so those smaller than unity are associated with noise-dominated eigenimages. The eigenvalues larger than unity are associated with dimensions with variance greater than the amplitude of the noise estimate. The break in slope near eigenvalues of 10 corresponds to a transition from spatially coherent to spatially incoherent eigenimages as shown in Figure 4. The thick black curve shows the distribution for the entire image shown in Figure 1. Increasingly thinner curves correspond to subimages 100, 30 and 15 pixels on a side. Spectral dimensionality diminishes with size of the subimage but there is significant variation in the dimensionality of subimages of the same size. The undeveloped areas in the upper left of Figure 1 have the lowest dimensionality while the developed areas in the lower right tend to have the highest dimensionality - at the range of scales considered here.*

Color image available from: *www.LDEO.columbia.edu/~small/Urban.htm*

reduction of variance (relative to the noise source) resulting from the smoothing operator. For the 5x5 and 11x11 gaussian filters, the rightward shift of the breakpoint in the eigenvalue distributions is accompanied by a corresponding increase in the number of spatially coherent eigenimages. For the 23x23 and 45x45 filters the breakpoint shifts back to lower dimensions and becomes less pronounced. Spatial smoothing attenuates variance at higher wavenumbers shifting the transition between the larger, more spatially coherent spectral features with higher variance and the succession of less spatially coherent features with lower variance. To the extent that some of this attenuated variance is noise, this is analogous to an increase in signal-to-noise ratio. Some of the attenuated variance would, however, be expected to correspond with actual spectral variability at the ~20m pixel scale. The larger filters may also be attenuating actual spectral endmembers and thereby reducing the dimensionality of the dataset and causing the breakpoint in the eigenvalue distribution to shift back to lower dimensions.

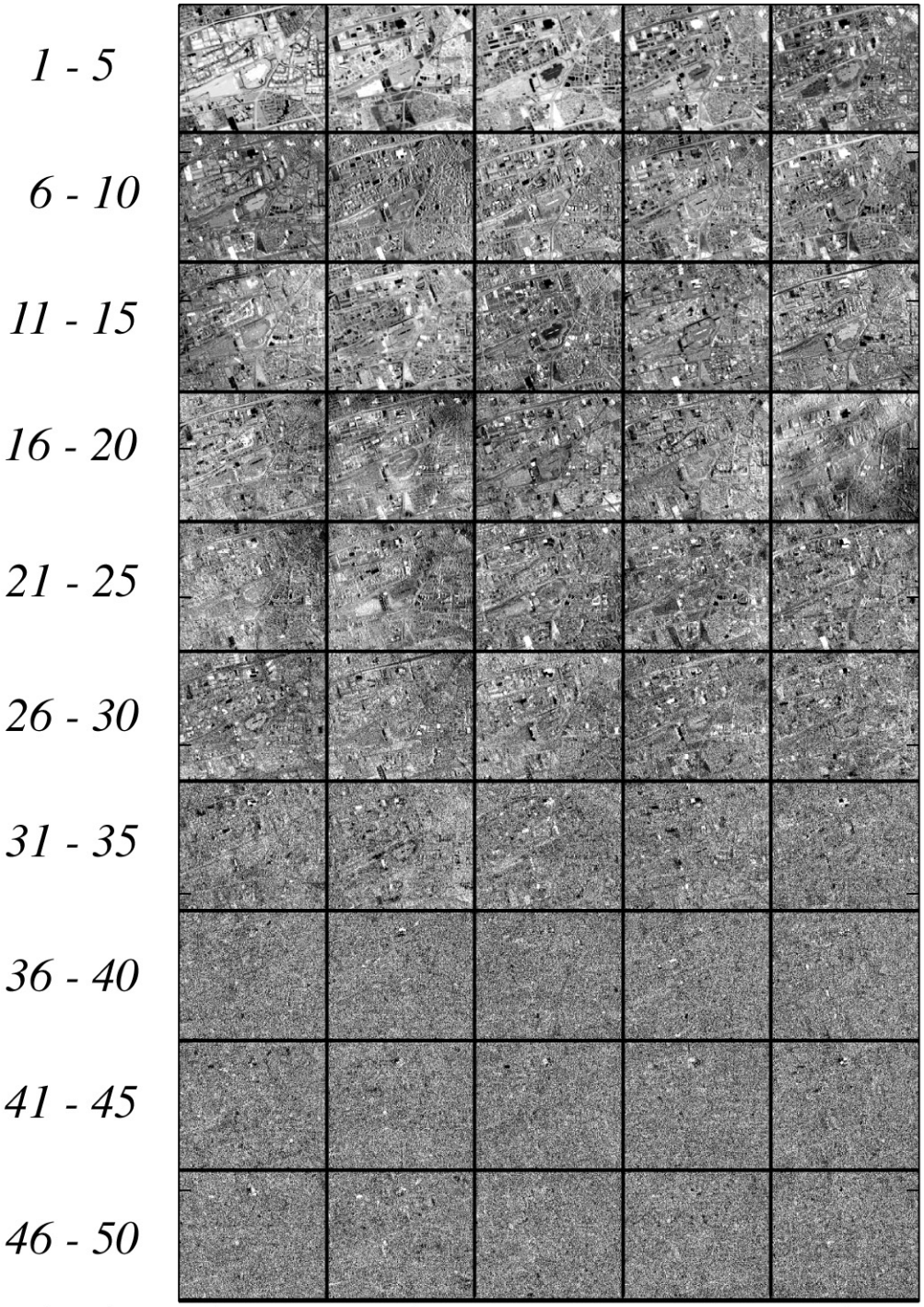

Figure 4. *Principal component images from a Minimum Noise Fraction (MNF) transformation of a subset of the AVIRIS image shown in Figure 1. The subset, from the lower right corner of Figure 1, contains residential, industrial and undeveloped areas. The transition from spatially coherent to spatially incoherent images occurs between 31 and 35 - consistent with the eigenvalues in Figure 3.*

Higher resolution image available from: *www.LDEO.columbia.edu/~small/Urban.htm*

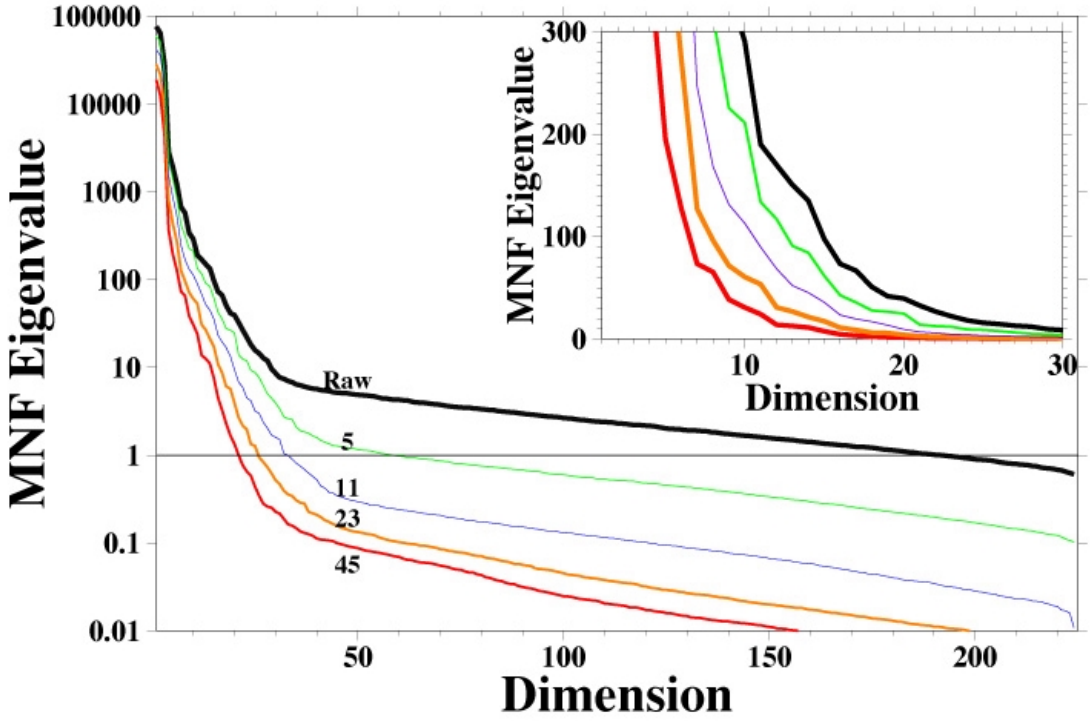

Figure 5. *Suppression of noise and dilution of spectral dimensionality. Spatial averaging with successively larger gaussian kernels simultaneously reduces both noise and information content at pixel scales. The 5x5 and 11x11 kernels increase the number of spatially coherent eigenimages and shift the breakpoint in the eigenvalue distribution to higher dimensions but the 23x23 and 45x45 kernels begin to attenuate some spectral endmembers and shift the breakpoint back to lower dimensions. Successively larger kernels attenuate increasing variance at high wavenumbers relative to the covariance of the noise estimate on which the MNF transformation is based.*

Color image available from: *www.LDEO.columbia.edu/~small/Urban.htm*

Spectral resampling results in appreciable loss of spectral dimensionality. The maximum dimensionality of the image is constrained by the number of spectral bands it contains. As would be expected, reducing the number of bands results in a direct loss of dimensionality without changing the signal-to-noise ratio in the remaining bands. Figure 6 indicates that subsampling by a factor of two significantly reduces the number of dimensions with variance greater than the noise estimate but does not change the breakpoint between the spatially coherent and spatially incoherent eigenimages. Subsampling the specra by a factor of four further reduces the spatially incoherent dimensions but also causes the breakpoint in the eigenvalue distribution to shift to a lower dimension. Resampling the spectra by factors of 8 and 16 has a pronounced effect on the dimensionality of the image - effectively eliminating some of the spectral dimensions and all but one or two spatially incoherent eigenimages. This reduces the number of spectral endmembers that can be represented uniquely. The loss of dimensionality occurs because many of the higher order spectral endmembers are characterized by subtle features that cannot be distinguished from one another without the fine spectral resolution provided by AVIRIS narrow spectral bandwidths.

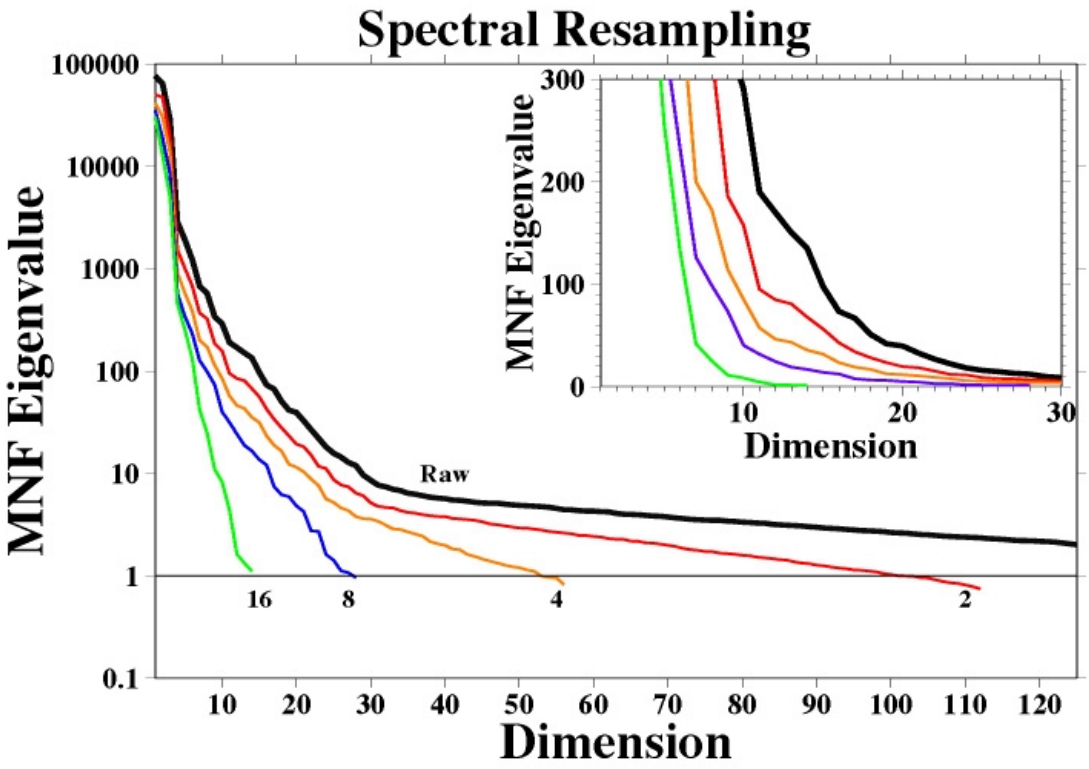

Figure 6. *Spectral resampling and loss of dimensionality. Resampling AVIRIS spectra by factors of 1/n for n= 2, 4, 8, and 16 rapidly reduces spectral dimensionality. Resampling by a factor of 1/4 results in some loss of significant dimensions as indicated by the leftward shift of the breakpoint in the eigenvalue distribution. Resampling by factors of 1/8 and 1/16 results in greater losses of spectral endmember resolution with spatially coherent eigenimages for all but the highest one or two dimensions.*

Color image available from: *www.LDEO.columbia.edu/~small/Urban.html*

Implications

The eigenvalue distributions have a consistent form for all of the subimages. They are all characterized by rapidly diminishing amplitude in the low order dimensions and a longer tail of gradually diminishing amplitude in the higher dimensions. When plotted in log-linear space, a distinct break in slope separates the two parts of the eigenvalue distribution. This transition between distinct log-linear eigenvalue distributions is analogous to that commonly observed in physical processes characterized by scaling relationships in the presence of noise processes. In this case, the low order eigenvalues are associated with spatially coherent eigenimages and the high order eigenvalues are associated with spatially incoherent eigenimages. Within the Milpitas study area, the spatially coherent eigenimages span approximately 30 spectral dimensions. The spectral endmembers associated with the extrema of the low order dimensions represent soil, vegetation, and a variety of high and low albedo anthropogenic endmembers. Despite the high spectral dimensionality of the urban mosaic, the low order dimensions with the highest spatial autocorrelations are associated with the hyperspectral equivalents of the spectral

endmembers that characterize broadband imagery of Milpitas and many other urban environments observed with Landsat and Ikonos imagery.

Variance at pixel scale represents a combination of noise and signal. The characteristic scale of urban reflectance is generally between 10 and 30 meters (*Small, 2001b*) so many of the 20-m AVIRIS pixels in the study area are likely to be spectral mixtures of at least two endmembers. This results in appreciable spectral variability at pixel scales and contributes to the higher order principal components whose eigenimages are not spatially coherent. Successive smoothing of the image suggests that apparent dimensionality increases somewhat as noise related variance is attenuated. More severe smoothing reduces apparent dimensionality as isolated spectral endmembers are attenuated. The first rotation applied by the MNF is based on the assumption that signal is strongly correlated among adjacent pixels and that noise is spatially uncorrelated at pixel scales. In urban environments where significant variations in reflectance occur at pixel scales, much of the pixel scale variance is not noise. Pre-rotation to diagonalize the noise covariance matrix therefore accommodates the spatially uncorrelated variance associated with the noise estimate but does not account for actual spectral variability at pixel scales. By ordering the resulting eigenimages by decreasing spatial autocorrelation, the MNF rotation emphasizes the spectral endmembers occurring at larger spatial scales and relegates the isolated and mixed spectra to the higher order dimensions. The scaling of eigenvalues in sigma noise units is convenient because it provides a benchmark for the amplitude of the instrument noise relative to pixel scale variance in the radiance field.

The apparent reduction in dimensionality with spatial scale is a consequence of the characteristic scales of the urban mosaic. The larger subimages generally contain a greater diversity of spectral endmembers and thus have higher dimensionality. The smaller subimages have higher dimensionality in residential suburbs and transitional areas and lower dimensionality in more spectrally homogeneous areas. In spite of the high spectral dimensionality of the urban mosaic, the majority of variance (97.5%) can be described with a four-endmember mixing model spanning the three low order dimensions of the mixing space. The consistency of endmembers suggests that the low dimensional projections of the mixing space resolved by broadband sensors does represent the true dominant endmembers even if they cannot represent the true spectral diversity of the urban mosaic. The scale analysis indicates that relatively high dimensionality is retained at least down to scales of 300 meters for high altitude AVIRIS in this area. Higher spatial resolution AVIRIS imagery may reveal higher spectral dimensionality at the same scales however. This method could also be used to quantify the spectral scaling properties of other environments. For instance, spatial scaling of reflectance spectral in forest canopies may provide insights into species diversity and forest succession dynamics.

Acknowledgments This work was funded, in part, by the Environmental Protection Agency - STAR program and the Columbia Earth Institute in association with the NASA SocioEconomic Data and Applications Center (SEDAC). The support of the Palisades Geophysical Institute and the Doherty Foundation is also gratefully acknowledged. Many thanks to Dave Hulslander for insights regarding ENVI's MNF algorithm.

References

Adams, J. B., M. O. Smith, and P. E. Johnson, Spectral mixture modeling; A new analysis of rock and soil types at the Viking Lander 1 site, *J. Geophys. Res.*, *91*, 8098-8122, 1986.

Adams, J. B., M. O. Smith, and A. R. Gillespie, Imaging Spectroscopy: Interpretation based on spectral mixture analysis. in Remote Geochemical Analysis: Elemental and Mineralogical Composition, edited by C.M. Pieters and P. Englert, 145-166, Cambridge University Press, New York, 1993.

Boardman, J. W. (1993). Automating spectral unmixing of AVIRIS data using convex geometry concepts. Fourth Airborne Visible/Infrared Imaging Spectrometer (AVIRIS) Airborne Geoscience Workshop, Jet Propulsion Laboratory, Pasadena, CA, p.11-14.

Boardman, J.W. and R.O. Green, Exploring the spectral variability of the earth as measured by AVIRIS in 1999, *Proceedings of the Ninth JPL Airborne Earth Science Workshop*, edited by R.O. Green,, Jet Propulsion Laboratory, Pasadena, CA, 195-206, 2000.

Boardman, J. W. and F. A. Kruse (1994). Automated spectral analysis: a geologic example using AVIRIS data, north Grapevine mountains, Nevada. Tenth Thematic Conference on Geologic Remote Sensing, Ann Arbor, MI, Environmental Research Institute of Michigan.

Gillespie, A. R., M. O. Smith, J. B. Adams, S. C. Willis, A. F. Fischer, and D. E. Sabol, Interpretation of residual images: spectral mixture analysis of AVIRIS images, Owens Valley, California, Proceedings of the 2nd Airborne Visible/Infrared Imaging Spectrometer (AVIRIS) Workshop, Pasadena, CA, 243-270, 1990.

Green, A. A., M. Berman, P. Switzer, and M. D. Craig, A transformation for ordering mutispecral data in terms of image quality with implications for noise removal, *I.E.E.E. Transactions on Geoscience and Remote Sensing*, *26*, 1, 65-74, 1988.

Green, R. O., and J. W. Boardman, Exploration of the relationship between information content and signal/noise ratio and spatial resolution in AVIRIS spectral data, *Proceedings of the Ninth JPL Airborne Earth Science Workshop*, edited by R.O. Green, Jet Propulsion Laboratory, Pasadena, CA, 195-206, 2000.

Landsberg, H. E., The Urban Climate. New York, Academic Press, 1981.

Research Systems Incorporated, ENVI 3.4 User's Guide, Boulder, CO, 930pp. 2000.

Small, C., Estimation of Urban Vegetation Abundance by Spectral Mixture Analysis, *International Journal of Remote Sensing*, *22*, 7, 1305-1334, 2001a.

Small, C., Multiresolution analysis of urban reflectance, *IEEE/ISPRS Conference on Remote Sensing of Urban Areas*, Rome, Italy, 2001b.

Smith, M. O., S. L. Ustin, J. B. Adams, and A. R. Gillespie, Vegetation in deserts: I. A regional measure of abundance from multispectral images, *Remote Sensing of Environment*, *31*, 1-26, 1990.

United, Nations, Prospects for Urbanization - 1999 Revision. United Nations, (ST/ESA/SER.A/166), Sales No. E.97.XIII.3, 1999.